Characterization of Woven Copper Mesh as a Heat Transfer Matrix at Low Temperatures

A. Onufrena[1, 2, 3], T. Koettig[1], T. Dorau[1], M. L. Laguna[1], J. Bremer[1], T. Tirolien[2], H. J. M. ter Brake[3]

[1] CERN, TE-CRG-CI, 1211 Geneva 23, Switzerland
[2] European Space Agency, ESA, 2200 AG Noordwijk, The Netherlands
[3] University of Twente, 7500 AE Enschede, The Netherlands

ABSTRACT

Woven metal mesh is a highly porous material that has a great potential as an internal structure for high-effectiveness compact counter-flow heat exchangers due to its large surface area and remarkably high transverse-to-axial conductivity ratio. This paper outlines an experimental characterisation and preliminary investigation into the use of copper mesh as a heat transfer matrix. The measurements of the thermal conductivity of the mesh in plane (45º to the fibres) and through-plane directions in the 10 to 300 K temperature range are presented. These data are used to determine the mesh residual resistivity ratio (RRR) and tortuosity as well as to estimate thermal conductivity in plane at 0º angle to the fibres. The temperature-dependent in- to through-plane conductivity ratio has reached values in the range of 10^3 - 10^4. The stress-strain profile of a 20-layer mesh stack was measured at 77 K and 290 K to further support the application of the stacked mesh layers. Moreover, the corresponding contact thermal conductance between copper mesh and different wall materials has been studied (copper, bronze, stainless steel) in the 10 to 300 K temperature range. Copper and bronze wall to copper mesh contacts were found to have the largest thermal conductance. Analysis and interpretations of all the obtained results are offered.

INTRODUCTION

Heat exchangers (HEXs) are the backbone of almost all thermodynamic cycles. In cryogenics it is a demanding technological barrier and its effectiveness can determine the performance of the entire system. Highly effective compact HEXs play a crucial role in Turbo-Brayton cryocoolers and in systems using the cryocooler-based fluid circulation approach [1, 2, 3]. Such circulation systems provide the cooling in the range between ≈ 2 W up to a few hundred watts at 4.5 K, which is not yet covered either by small or large scale cryogenic installations [4]. The applications that can greatly profit from the cooling powers in this range include infrared cameras and spectrometers in space missions, highly sensitive SQUID magnetometers [5] used in particle accelerator and medical applications, cryogenic mirrors of gravitational wave detectors and low-temperature experimental platforms.

The performance of a compact cryogenic HEX will be heavily dictated by the choice of its internal geometry. The targeted geometry features to achieve high effectiveness are compactness and large area of the internal surface accompanied by high heat transfer coefficients. Moreover, for

Cryocoolers 21, edited by R.G. Ross, Jr., J.R. Raab and S.D. Miller

cryogenic designs where the temperature gradients along the HEXs tend to be large, longitudinal conduction along the structure can contribute to the performance deterioration [6]. For that reason, the inner heat transfer geometries made of materials with non-uniform thermal conductivity (namely low in the direction of the flow and high across it) can be of great interest.

Woven copper mesh formed of layers of intertwined wires is often used as a matrix structure in the cryocooler cold heads [7]. Due to its high wetted surface area per volume, heat transfer coefficient, high thermal conductivity and ease of manufacturing, it presents an interesting candidate for the HEX heat transfer matrix [8, 9]. Moreover, a woven mesh stack has a high number of wire-to-wire interfaces across its height, presenting a thermal resistance to the heat flow across the mesh layers, helping to hinder the aforementioned longitudinal conduction and provide the necessary non-uniform thermal conductivity required to achieve the high performance.

Several attempts were made to characterize the thermodynamic properties and suitability of the mesh as a heat transfer media numerically. A few mesh-based HEX designs were accomplished experimentally [8, 9]. However, experimental data describing critical properties (e.g. mesh thermal conductivity, elastic properties and associated thermal contact conductance) that are necessary to accomplish effective mesh-based HEX design as well as to assure the confidence in the numerical models have not yet been presented.

This paper outlines an evaluation of the thermal and mechanical properties of the woven copper wire mesh relevant to the cryogenic mesh-based HEX design based on numerous experimental studies. These include the experimental measurements of in- and through-plane thermal conductivity of the mesh under different mechanical load conditions in the 11 to 290 K range, the stress-strain behavior for low compression forces at 77 and 290 K as well as the studies of the mesh-to-copper, mesh-to-stainless steel and mesh-to-bronze thermal interface conductance down to 11 K. It was shown that the latter plays an important role in the performance of the mesh-based HEXs [1]. Further analysis of the experimental results, e.g. evaluation of the elasticity moduli and tortuosity, is presented and an interpretation is proposed.

EXPERIMENTAL INVESTIGATIONS

To accomplish a highly effective mesh-based HEX design, thermal conductivities of the copper mesh in transverse (in-plane) and in axial (through-plane) directions should be known as these are essential for the evaluation of the heat transfer across and along the HEX structure. The longitudinal heat transfer is especially important as it can result in a serious performance deterioration for compact cryogenic HEXs [6]. It will be seen later that the mesh through-plane conductivity depends on the compression between its layers. Thus, to achieve the desired HEX performance the characterisation of the stress-strain behavior of the mesh is necessary. Within the HEX, the mesh will inevitably be in thermal contact with other materials. Thermal conductance of this contact has a strong influence on the effectiveness of a mesh-based HEX [1], thus it is important to characterize it for the relevant materials.

The following subsections will highlight the experimental studies and theoretical evaluations that were performed to characterise the aforementioned properties of the copper mesh down to lower temperatures, e.g. thermal conductivity in transverse and axial directions, stress-strain behavior and thermal conductance of the mesh-metal contacts.

Thermal conductivity of the copper mesh

To measure transverse conductivity of the mesh down to cryogenic temperatures, the mesh sample was mounted on the 2nd stage of a 1 W @ 10 K Gifford-McMahon (GM) cryocooler as shown in Figure 1a. The sample was equipped with a heater (top, EH_1) and two calibrated TVO temperature sensors (T_1 and T_2). Clamps, thermal grease and indium foil were used to improve thermal contacts between the instrumentation and the sample. For a given stage temperature T_i regulated by an additional heater, the conductivity $\lambda_{||,i}$ can be deduced experimentally via:

$$\lambda_{||,i} = \frac{\dot{Q}_{EH1} \cdot L}{(T_1 - T_2) \cdot A} \tag{1}$$

where $\dot{Q}_{EH1}$ is the heater power, L is the distance between the temperature sensors, A is the cross-sectional area of the sample as shown in Figure 1a. The cryocooler stage temperature was controlled using an additional heater (EH_2). For stage temperatures above 60 K, thermally insulating glass fibre

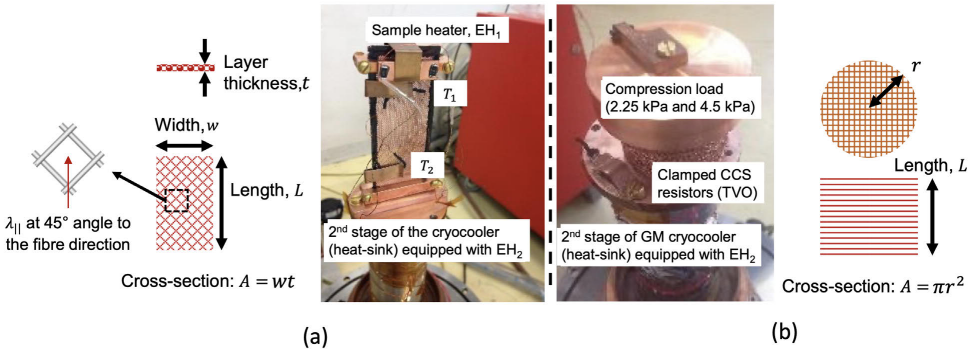

Figure 1. Test setup for the measurement of transverse (a) and axial (b) thermal conductivity of copper mesh with the corresponding length and area used in the calculations. Samples are made of OFHC copper. Dimensions: wire diameter = 315 μm, mesh size = 815 μm.

composite (G10) layers were used to limit the thermal contact between the stage and the sample, hence reducing the heating power required to bring the sample to the higher temperatures.

To improve the measurement accuracy, the TVO sensors were calibrated against each other in the 11 to 300 K range. The temperature offset between the sensors was measured at steady temperatures under $\dot{Q}_{EH1} = 0$ W condition and was used as a correction in the conductivity calculations. The mesh sample was mounted such that the heat was transferred at a 45° angle with respect to the wire direction as shown in Figure 1 and there is no mesh wire directly linking the two temperature measurement positions. This way the lowest $\lambda_{||}$ is measured, ensuring the most conservative in-plane conductivity assumption for the future HEX designs.

The measured transverse (45° angle) conductivity profile is presented in Figure 2. It is similar to that of a bulk copper with a characteristic peak around 25 K where $\lambda_{||} \approx 260$ W/mK is reached. The conductivity in this region is affected by the purity of the copper, porosity of the mesh and the tortuosity of the wires. The latter is defined as a modification of the conduction path due to the presence of the interfaces between the wires and their curved structure. It lies between 0% and 100% with 100% representing a non-porous bulk material. To assess the purity of the copper in the mesh wires (e.g. their RRR) and quantify

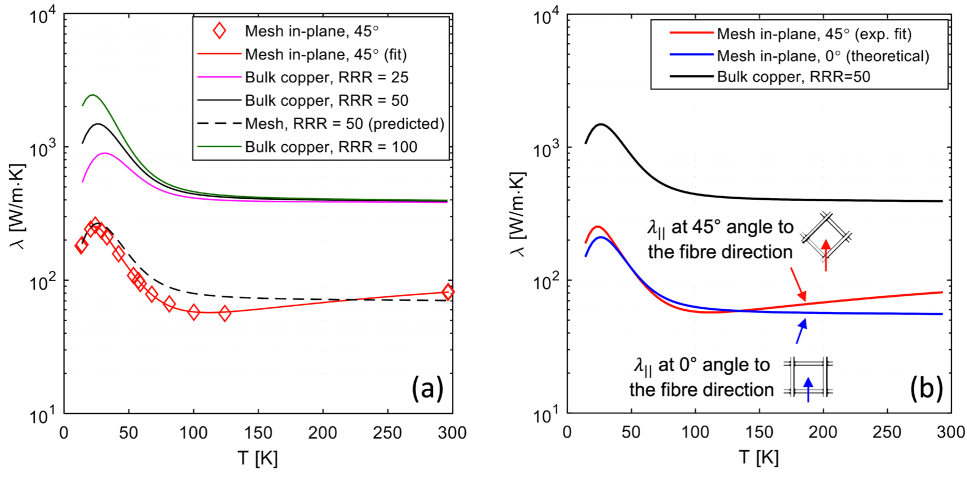

Figure 2. Transverse thermal conductivity variation with temperature. (a) Measured mesh conductivity at 45° angle to the fibre direction is compared to that of the bulk copper and RRR = 50 copper normalized profile. (b) Mesh conductivities at 45° angle (measured) and 0° (calculated) to the fibres compared to that of the bulk copper with RRR = 50. Mesh dimensions: wire diameter = 315 μm, mesh size = 815 μm. Measurement uncertainty: 0.05 - 0.4 K (temperature); 5% - 18% (thermal conductivity).

the tortuosity, the analysis presented by Tomas et al. [10] can be adapted to the case of the mesh. For a porous geometry of the mesh, the transverse thermal conductivity can then be expressed via:

$$\lambda_{||} = \lambda_{Cu-wire}(1 - e_v)\tau \quad (2)$$

where λ_{Cu} is the conductivity of the copper in the mesh wires, e_v is the porosity and τ is the tortuosity of the sample expressed as a value between 0 and 1. From eq. (2) it follows that the ratio $\lambda_{\|}/\lambda_{Cu\text{-}wire}$ only depends on the sample geometry and thus must be constant throughout the 10 to 300 K temperature range. $\lambda_{\|}/\lambda_{Cu\text{-}wire}$ can be determined from the measured mesh conductivity profile and that of copper in the wires. However, the latter depends on its RRR and is unknown. Luckily, in the 200 to 300 K region the thermal conductivity of the bulk copper is independent of the RRR and it is at a relatively constant value of 400 W/m·K. Thus from the measured conductivity of the mesh in this region, $\lambda_{\|}/\lambda_{Cu} = 0.16$ was found.

At lower temperatures the conductivity of copper is no longer independent of RRR. However, as $\lambda_{\|}/\lambda_{Cu} = 0.16$ has to stay constant, the peak conductivity of the copper wires can be determined from the peak conductivity of the mesh. The peak $\lambda_{Cu\text{-}wire}$ at around 25 K was found to be ≈ 1500 W/mK, corresponding to RRR ≈ 50 of the copper wires.

The porosity of the sample was measured to be 62%. From eq. (2), the tortuosity of 41% can now be deduced. For a homogeneous copper sample of similar porosity τ = 55% was measured [10]. The lower value of our mesh sample confirms that the heat path in the mesh sample experiences more obstruction due to the presence of the interfaces between the copper wires. Based on the RRR = 50 and the tortuosity of the copper in the wires of 41%, the theoretical mesh conductivity profile that can be obtained based on eq. (2) and is shown in Figure 2a. The predicted profiles shows a good agreement with experimental data.

The thermal conductivity of mesh at 0º angle to the wires can be approximated based on that of copper with RRR = 50, total conduction area occupied by the wires along the sample and increase in their effective length due to the woven structure of the mesh. In this analysis, it was assumed that only the wires at 0° angle (and not those at 90° angle) to the measurement direction are contributing to the heat conduction. Their waviness was found to result in an increase of 7% in the wire length compared to the mesh sample dimensions (see Figure 1). The final predicted mesh conductivity profile at 0° to the fibres is depicted in Figure 2b. One can see that the values are approximately equal to those from the 45° angle to fibre direction. Even though wire-wire interfaces do not interrupt the heat path in 0° angle measurement case, the total area of the wires transporting the heat is reduced, thus no increase in the conductivity value is observed. This prediction needs to be confirmed by experimental measurements. For axial conductivity measurements, a 10-layer stack was mounted on the 2nd stage of the cryocooler as shown in Figure 1b. A copper block of a known mass was placed on top of the stack to ensure the constant compression force between the mesh layers throughout the test. The same measurement principle was applied as in the case of the transverse thermal conductivity test. The two temperatures for axial conductivity evaluation were measured on the copper mass and the 2nd stage of the cryocooler using clamped TVO sensors and the cross-sectional area as shown in Figure 1b was used.

The measured conductivity values in axial direction under 2.25 kPa and 4.5 kPa compression loads together with these in transverse direction at 45º angle to mesh fibres are compared in Figure 3. In axial direction, the two contributors to mesh thermal conductivity are the bulk conduction across the copper wires and the thermal conductance of the point contacts between the wires. Due to the high number of wire-wire interfaces, the thermal conductivity is dominated by the second contribution and is significantly lower than the one in the transverse direction. Thermal contact conductance worsens at lower temperatures as will be shown further, which explains the absence of an evident conductivity peak in axial direction. Based on the data from Figure 3, the ratio of transverse-to-axial thermal conductivity of 10^3-10^4 can be deduced. Moreover, from the test data for 2.25 kPa and 4.5 kPa loads one can conclude that it increases with the compression force by an approximately constant factor of ≈ 2 over the covered temperature range.

These test results confirm that the woven copper mesh can make a great candidate for the inner structure of a cryogenic HEX. It offers a unique advantage of decoupling the thermal conductivity along and across the matrix, thus the conduction between the warm and cold ends of the heat exchanger can be minimized and its performance can be improved.

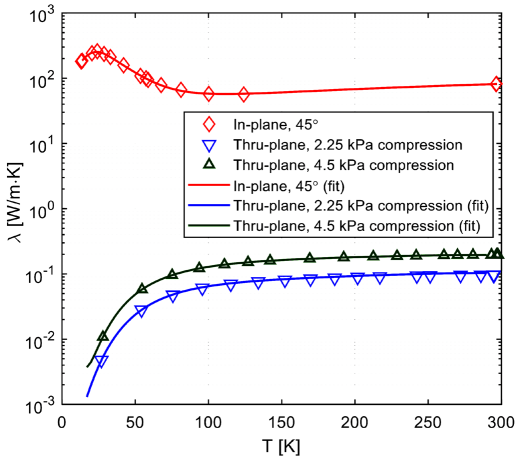

Figure 3. Temperature-dependent thermal conductivity of the mesh in transverse direction and through-plane direction under 2.25 kPa and 4.5 kPa compression loads. Mesh dimensions: wire diameter = 315 μm, mesh size = 815 μm. Measurement uncertainty: 0.05 K - 0.4 K (temperature); 12% - 20% (thermal conductivity).

The axial ($\lambda_\perp$) and in-plane ($\lambda_{||}$) conductivity fits for this range of temperatures T are proposed by eqs. (3) and (4) and included in Figure 3:

$$log_{10}\,\lambda_\perp = a_0 + a_1 \cdot log_{10}\,T + a_i \cdot (log_{10}\,T)^i + \cdots + a_n \cdot (log_{10}\,T)^n \tag{3}$$

$$\lambda_{||} = 0.76/(W_o + W_i + W_{io}) \tag{4}$$

where coefficients W_o, W_i and W_{io} are defined as:

$$W_o = b_0/T \tag{5}$$

$$W_i = b_1 \cdot T^{b_2}/(1 + b_1 \cdot b_3 \cdot T^{b_2+b_4} \cdot e^{-b_6 \cdot (b_5/T)}) \tag{6}$$

$$W_{io} = b_7 \cdot W_i \cdot W_o/(W_i + W_o) \tag{7}$$

with the coefficients and as given in Table 1.

Stress-strain behavior of the copper mesh

As it follows from the previous section, mesh has a remarkably high transverse-to-axial conductivity ratio. However, as seen from Figure 3 the axial conductivity of the mesh is sensitive to and increases with the compression force between the mesh layers, even under low compression loads (e.g. 4.5 kPa). To maintain the low axial thermal conductivity of the mesh and to ensure that the desired weak contact between the wires is maintained during the HEX assembly, the stress-strain behavior of the mesh should be characterized.

Table 1. Coefficients for copper mesh thermal conductivity fits as defined in eqs. (3) - (7).

i	a_i (for 2.5 kPa load)	a_i (for 4.5 kPa load)	b_i
0	-1.999	2.2	5.500×10^{-2}
1	-1.999	-37.5	1.364×10^{-9}
2	-2.000	272.1	3.818
3	1.761	-1119.4	2.397×10^{1}
4	2.000	2859.9	4.491×10^{-1}
5	-0.444	-4656.4	2.597×10^{2}
6	-1.278	4723.3	-1.064×10^{-4}
7	0.692	-2726.1	2.001
8	-0.101	680.9	0.000

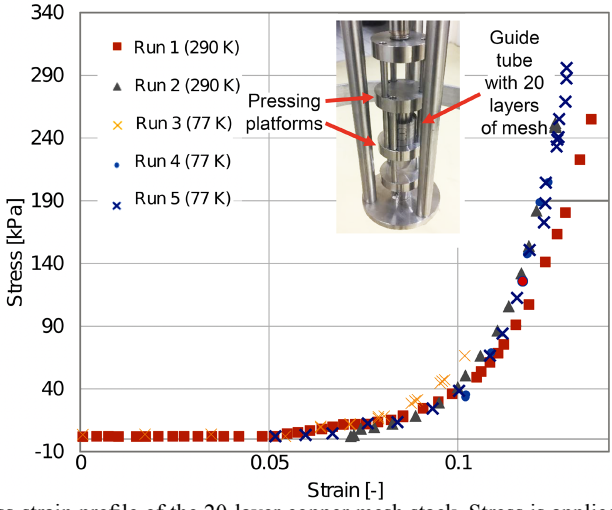

Figure 4. Stress-strain profile of the 20-layer copper mesh stack. Stress is applied to a circular cross-section of mesh with 40 mm diameter. Mesh dimensions: wire diameter = 315 μm, mesh size = 815 μm. The maximum measurement uncertainties: ±1.5% (stress), ±8.7% (strain).

For the experimental test, the stack of 20 mesh layers was placed in a guide tube and mounted between two pressing platforms in a traction machine as shown in Figure 4. The compression loads up to 300 kPa were exerted and the displacement from the initial position of the platform was recorded using a Linear Variable Differential Transformer sensor. The test runs at 290 and 77 K were performed to evaluate the stress-strain profiles depicted in Figure 4.

The measured values are very far from the ≈ 200 MPa elastic limit of the bulk copper, suggesting that the compression is mainly due to the spring-like nature of woven mesh. The observed profile is not linear and at low compression loads the measured strains are large, which might be due to the movement of the mesh fibres. From the higher strain regions, the elasticity modulus of the mesh can be approximated to lie in the 9 - 13 MPa range at 290 K and 11 - 20 MPa range at 77 K.

Thermal contact conductance between the copper mesh and bulk metals

To characterise thermal conductance of the mesh-metal contacts, the setup depicted in Figure 5 was used. The test specimen consists of two concentric tubes (further also referred to as "walls"for the heat-transfer description purposes) with the copper mesh annuli placed between the tubes. Such geometry is chosen to better represent a frequently used concentric heat exchanger configuration [1, 8]. The outer tube is in thermal contact with the 2nd stage of the cryocooler and its temperature is controlled using the corresponding heater EH_{cc2} (see Figure 5a and 5b). Several layers of thermally insulating G10 panels are placed between the 2nd stage of the cryocooler and the sample to allow reaching higher outer tube temperatures. The inner tube is made out of the test material of interest and is only in contact with the copper mesh. The specimen is equipped with a sample heater EH_{sample} and two calibrated TVO temperature sensors measuring the temperatures T_1 and T_2, all at the locations indicated in Figure 5b and 5c. Temperature sensors are pressed to the inner and outer tubes using Indium foil. Apiezon grease is used to ensure a good thermal contact between the surfaces and the heaters. For a heat Q applied to the inner tube, the mesh-tube thermal contact conductance coefficient at a given temperature can be calculated based on:

$$\dot{Q} = \Delta T \cdot \left(\frac{s_{w1}}{\lambda_{w1} A_{w1}} + \frac{1}{\alpha_{c1} A_{c1}} + \frac{ln(d_{out}/d_{in})}{\lambda_{mesh} \cdot 2\pi L} + \frac{1}{\alpha_{c2} A_{c2}} + \frac{s_{w2}}{\lambda_{w2} A_{w2}} \right)^{-1} \quad (8)$$

where the temperature difference $\Delta T = T_1 - T_2$, L is the height of the mesh stack, s_{w1} and s_{w2} are the thicknesses, d_{in} and d_{out} are the diameters, and A_{w1} and A_{w2} are the conduction areas of the inner and outer tubes, respectively and $A_{w1} = \pi d_{in} L$ and $A_{w2} = \pi d_{out} L$ assuming thin walls. A_{c1} and A_{c2} are the

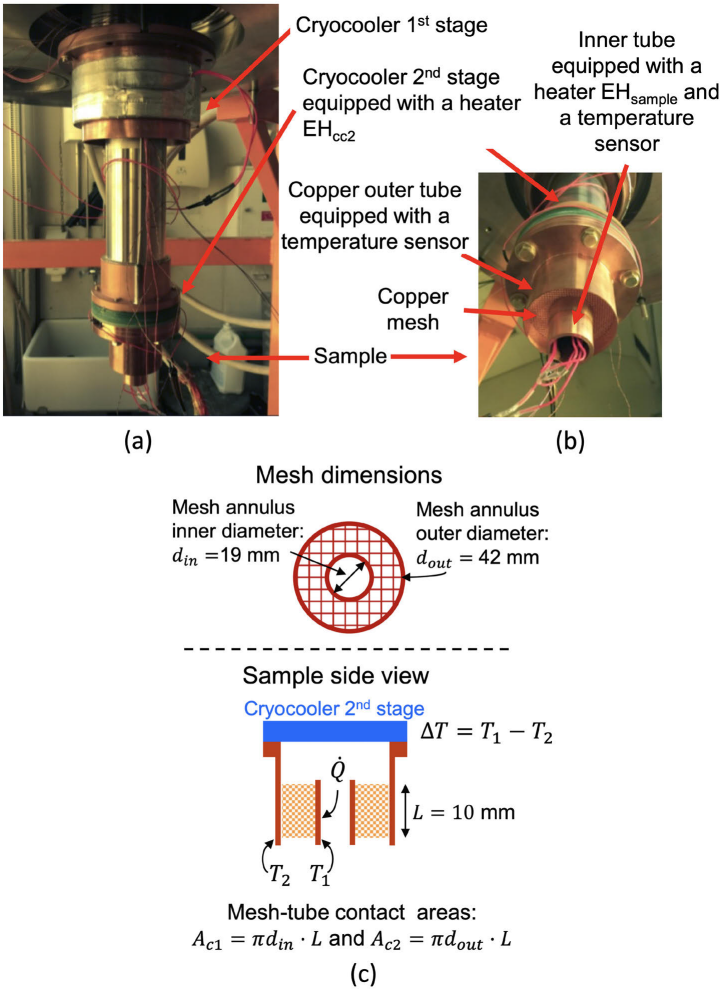

Figure 5. Setup for the measurement of thermal contact conductance between copper mesh and various inner tube materials. (a) Specimen mounted on the cryocooler. (b) Detailed view of the specimen. (c) Schematic representation of the sample with relevant dimensions and heating and temperature measurement locations. Mesh dimensions: wire diameter = 315 µm, mesh size = 815 µm.

respective mesh-to-inner and mesh-to-outer tube contact areas calculated as shown in Figure 5c. λ_{w1}, λ_{w2} and λ_{mesh} are the known temperature-dependent tube and mesh conductivities (see Figure 2 for λ_{mesh} values). Similarly to the mesh thermal conductivity measurements, ΔT was corrected for the offset between the sensors that was measured for $\dot{Q} = 0$ in the given test configuration over the entire temperature range, allowing to reduce the measurement uncertainty.

The sample dimensions are shown in Figure 5c. Copper was chosen as an outer tube material to ensure a more homogeneous temperature T_2 distribution. For certain inner tube materials used in the test (e.g. bronze and stainless steel), an additional copper insert was brazed onto the inner surface of the tube to ensure uniform application of the heat $\dot{Q}$.

The thermal contact conductance coefficients were measured for the contacts between copper mesh and three different inner tube materials: copper, bronze and stainless steel. The thermal conductance coefficient α_{c2} between the outer copper tube and the mesh could be calculated from the test where the inner copper tube is used, e.g. $\alpha_{c1} = \alpha_{c2}$, assuming the force between the mesh wires in contact with the tubes is equal (see further paragraphs for justification). Based on this value, α_{c1} could be calculated for mesh-to-bronze and mesh-to-stainless steel thermal contacts.

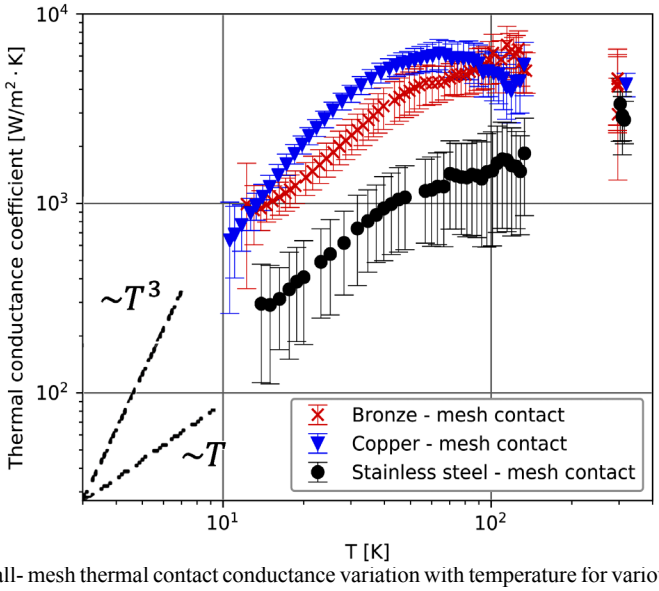

Figure 6. Wall- mesh thermal contact conductance variation with temperature for various wall materials: bronze, stainless steel and copper. Mesh dimensions: wire diameter = 315 μm, mesh size = 815 μm. Temperature measurement uncertainty: 0.05 K - 0.4 K (horizontal error bars are not shown for clarity).

Thermal contact conductance coefficients deduced from the measurements in the 11 to 130 K range as well as at 300 K are presented in Figure 6. For metal-metal contacts the conductance at lower temperatures is expected to increase according to a T^n dependency. The linear profile, e.g. $n = 1$, is observed in the pure or lightly oxidized metallic contacts, whereas $1 < n < 2$ is applicable for oxidized metals and varies depending on surface impurities and roughness [11, 12]. A value $n = 3$ represents a contact with an insulating material. Temperature lines proportional to T and T^3 are shown for a reference in Figure 6. It can be seen here that the experimental data follows T^n dependencies with $n = 1.2$ - 2 suggesting the presence of the oxide layers on the metals in question as expected. The mesh-to-copper and mesh-to-bronze contacts were found to be more conductive than mesh-to-stainless steel contact similarly to the trends observed in literature [11]. This result can be explained by the presence of available free electrons for the heat transfer in copper mesh, copper and bronze as well as the higher thermal conductivity of these materials compared to the stainless steel. For mesh-to-stainless steel contact, the passivated oxide layer presents a barrier for the heat transfer, thus its thermal conductance is worse. A slight thermal conductance peak for mesh-to-copper interface can be observed similarly to that in Figure 2 for the copper mesh, suggesting the wire-to-wire contact conductance is of a similar magnitude as that of the mesh-to-copper.

As the temperature increases, the contact conductance growth slows down gradually and the value becomes almost constant at higher temperatures [11]. As no large change in conductivity is expected at higher temperatures, the conductance values were measured only up to 130 K and at around 300 K.

Thermal contact conductance is sensitive to and increases with the compression force. The compression is assumed to be equal for the three contacts in Figure 6. This was ensured by carefully maintaining the sample dimensions throughout the tests. The mesh layers were machined using electro-erosion process yielding the ±30 μm diameter accuracy with respect to the inner and outer tubes. For the mesh dimensions used in the test, the maximum contact pressure of 9.6 MPa between the mesh wires and the inner tube was approximated analytically [1]. However, at lower temperatures the copper mesh becomes stiffer and is subject to thermal dilatation. The influence of these factors and hence the exact value of the compression force between the mesh and the inner tube is difficult to estimate due to a non-trivial geometry of the mesh.

Nevertheless, to approximate the mesh-wall contact compression range, the experimental findings from Figure 6 can be compared to those from the literature sources. An extensive review of

contact conductance data for a range of contact pressures and temperatures was accomplished by Gmelin et al. [11]. For the purpose of this comparison, mesh-to-copper contact is approximated with that of a Cu-Cu, mesh-to-bronze with Cu-brass and mesh-to-stainless steel with Cu-stainless steel contacts, respectively. Using linear interpolation between the data from the references 16a, 16b and 63a [11] in the 10 to 130 K range, the conductance of a Cu-Cu contact can be approximated to lie within the 220 - 1900 $m^2 \cdot K$ range for up to 3.8 MPa compression loads. From Figure 6 it follows that the measured values for mesh-to-copper contact conductance are in the 650 - 6480 $W/m^2 \cdot K$ range that is approximately three times higher. This suggests the contact pressure between the mesh and the tube is above 3.8 MPa. At ≈ 300 K the contact conductance of about 4300 $W/m^2 \cdot K$ was measured for mesh-to-copper and mesh-to-bronze contacts and around 3000 W/m^2K for mesh-to-stainless steel contact. The corresponding literature values in the 1 MPa - 3.8 MPa compression range were found to be lower, e.g. Cu-brass: 1430 $W/m^2 \cdot K$ at 362 K (ref. 59b), Cu-Cu: 3700 $W/m^2 \cdot K$ at 300 K (ref. 63a) and Cu-INOX: 835 $W/m^2 \cdot K$ at 388 K (ref. 59c) [11]. All this implies that the compression for the contacts depicted in Figure 6 is above 3.8 MPa and lies in the 3.8 to 9.6 MPa range.

Within the context of cryogenic heat exchangers, there can be a high interest in increasing the thermal conductance of the mesh-solid contact [1]. It can be achieved with a higher compression force at the contact in question. Further improvement can be gained by soldering or brazing the mesh to a solid surface using intermediate material layers. However, the longitudinal conduction of materials used for the brazing can have additional implications on the performance of high-effectiveness cryogenic heat exchangers further outlined in literature [1].

CONCLUSIONS

Thermal, mechanical and electrical properties of the woven copper mesh relevant for its use as a heat transfer medium in compact high-effectiveness cryogenic heat exchangers were characterized experimentally.

Thermal conductivity of the copper mesh was measured in transverse in-plane direction at 45° angle to the mesh fibres and in axial through-plane direction. The in-plane measurements showed that the mesh conductivity profile is similar to that of the bulk copper with a characteristic peak towards lower temperatures reaching 250 W/mK. From these data, the analysis was performed to estimate the tortuosity of the mesh to lie around 41% and the purity of the mesh wires correspond to RRR ≈ 50. Based on these findings, the conductivity of the mesh at 0° angle to the fibres was estimated to lie close to that in transverse 45° angle direction. This estimate should be confirmed experimentally. From the through-plane measurements under 2.25 kPa and 4.5 kPa loads, it was concluded that doubling the compression force approximately doubles the axial thermal conductivity of the mesh. This increase is due to the higher thermal conductance of the wire-wire interfaces. Overall, the ratio 10^3 - 10^4 of transverse-to-axial thermal conductivities was observed during the tests in the 11 to 300 K range. Such thermal decoupling in the two directions can bring a significant reduction of axial conduction along a mesh-based heat exchanger. The stress-strain behavior of the mesh was also characterized with the elasticity moduli approximated to lie between 9 MPa and 20 MPa in the 77 to 290 K range.

Thermal conductance of the contact between the copper mesh and three solid materials, namely copper, bronze and stainless steel was measured between 11 to 300 K. The low temperature behavior was consistent with the literature data following T^n dependency with n = 1.2 - 2. Mesh-to-bronze and mesh-to-copper contacts were found to be more conductive than mesh-to-stainless steel contact. After comparison with the literature data, the mesh-to-metal contact compression was estimated to lie in the 3.8 to 9.6 MPa range. Since a higher thermal contact conductance might be of interest for cryogenic heat exchanger designs [1], soldering or brazing of the inner tube to the mesh is suggested.

In conclusion, based on the measured properties we identify mesh as a promising material for the inner structure of the high-effectiveness compact cryogenic heat exchangers. Its high heat transfer area and highly non-uniform thermal conductivity in the two directions satisfy the most desired characteristics of an excellent heat transfer matrix.

ACKNOWLEDGMENTS

This research was performed within the CERN Cryolab in collaboration with the European Space Agency (ESA). Institutional support of both CERN and ESA is greatly appreciated by the authors of this article.

REFERENCES

1. Onufrena, A., T. Koettig, J. Bremer, T. Tirolien, T. Dorau, M. B. Laguna, H.J.M ter Brake, "Design of a compact mesh-based high-effectiveness counter-flow heat exchanger," *Cryogenics,* (to be submitted).
2. Onufrena, A., T. Koettig, J. Bremer, T. Tirolien, T. Dorau, M. B. Laguna, H.J.M ter Brake, "Recuperator for 40 K Reverse Turbo-Brayton Cooler and Remote Cooling Applications," *European Space Thermal Engineering Workshop,* (2020).
3. Tanchon, J., J. Lacapere, A. Molyneaux, M. Harris, S. Hill, S.M. Abu-Sharkh, T. Tirolien, "A Turbo-Brayton Cryocooler for Future European Observation Satellite Generation," *Cryocoolers 19*, ICC Press, Boulder, CO (2016), pp. 437-446.
4. Decker, L., "Overview on cryogenic refrigeration cycles for large scale HTS applications," *International Cryogenic Engineering Conference*, (2016).
5. Rijpma, A.P., C.J.H.A. Blom, A.P. Balena, E. de Vries, H.J. Holland, H.J.M. ter Brake, H. Rogalla, "Construction and tests of a heart scanner based on superconducting sensors cooled by small Stirling cryocoolers," *Cryogenics*, Vol. 40, Issue 12 (2000), pp. 821-828.
6. Barron, R. F., Gregory F. Nellis, "Cryogenic Heat Transfer," *Chemical and Mechanical Engineering,* CRC Press (1999).
7. T. Koettig, "Dünnschichtsysteme für die effektive Tieftemperaturregeneration," (2008).
8. Steyert, W A, Stone, N J., "Low flow velocity, fine-screen heat exchangers and vapor-cooled cryogenic current leads," (1978).
9. H. Zhao, Y. Hou, X. Su, and Q. Zhang, "Performance analysis of woven wire screen matrix heat exchanger units," *Journal of Thermal Science and Technology*, Vol. 6, No. 1 (2011), pp. 192-202.
10. Tomas, G., D. Martins, A. Cooper, G. Bonfait, "Low-temperature thermal conductivity of highly porous copper," *Cryogenic Engineering Conference*, (2015).
11. Gmelin. E, M. Asen-Palmer, M. Reuther, R. Villar, "Thermal boundary resistance of mechanical contacts between solids at sub-ambient temperatures," J*ournal of Physics D: Applied Physics*, Vol. 32, no.6 (1999).
12. Dhuley. R, C., "Pressed copper and gold-plated copper contacts at low temperatures – A review of thermal contact resistance," *Cryogenics*, Vol. 101 (2019), pp. 111-124.